Noncanonical Wnt signaling regulates midline convergence of organ primordia during zebrafish development

Takaaki Matsui, Ángel Raya, Yasuhiko Kawakami, Carles Callol-Massot, Javier Capdevila, Concepción Rodríguez-Esteban, and Juan Carlos Izpisúa Belmonte[1]

Gene Expression Laboratory, The Salk Institute for Biological Studies, La Jolla, California 92037, USA

Several components of noncanonical Wnt signaling pathways are involved in the control of convergence and extension (CE) movements during zebrafish and *Xenopus* gastrulation. However, the complexity of these pathways and the wide patterns of expression and activity displayed by some of their components immediately suggest additional morphogenetic roles beyond the control of CE. Here we show that the key modular intracellular mediator Dishevelled, through a specific activation of RhoA GTPase, controls the process of convergence of endoderm and organ precursors toward the embryonic midline in the zebrafish embryo. We also show that three Wnt noncanonical ligands *wnt4a*, *silberblick/wnt11*, and *wnt11-related* regulate this process by acting in a largely redundant way. The same ligands are also required, nonredundantly, to control specific aspects of CE that involve interaction of Dishevelled with mediators different from that of RhoA GTPase. Overall, our results uncover a late, previously unexpected role of noncanonical Wnt signaling in the control of midline assembly of organ precursors during vertebrate embryo development.

[*Keywords*: Heart; endoderm; noncanonical Wnt signaling; Dishevelled; RhoA]

Supplemental material is available at http://genesdev.org.

Received August 24, 2004; revised version accepted October 25, 2004.

During embryonic development in vertebrates, precursor cells of many organs initially appear as bilateral populations of cells that subsequently migrate toward the embryonic midline, where they assemble to form the primitive organs. For example, myocardial precursors appear bilaterally in the anterior lateral plate mesoderm and migrate toward the midline, where they assemble to form a primitive heart tube in all vertebrates analyzed so far (for review, see Stainier 2001). Similar events determine the formation of primitive foregut structures including duodenum, liver, and pancreas (Warga and Nusslein-Volhard 1999; Ober et al. 2004). In the case of heart tube assembly, genetic screens in zebrafish have identified eight mutations that disrupt this process, resulting in the formation of two laterally positioned hearts (a phenotype known as cardia bifida; Chen et al. 1996; Stainier et al. 1996). Analyses of these mutations have pinpointed several requirements for heart tube assembly (for review, see Stainier 2001): (1) correct differentiation and morphogenesis of myocardial precursors, since mutations that impair myocardial differentiation (*faust* and *hands off*) or epithelial polarity of myocardial precursors (*natter*) are associated with cardia bifida phenotypes (Reiter et al. 1999; Yelon et al. 2000; Trinh and Stainier 2004); (2) correct endoderm specification, since mutant embryos that lack endoderm (*bonnie and clyde*, *casanova*, *faust*, and *one-eye pinhead*) also display cardia bifida (Schier et al. 1997; Alexander et al. 1999; Reiter et al. 1999; Kikuchi et al. 2000); and (3) a still unclear mechanism that disrupts intrinsic properties of myocardial migration, affected in *miles apart* mutant embryos, in which myocardial differentiation and endoderm specification are otherwise normal (Kupperman et al. 2000). Endodermal cells also migrate toward the midline to form the primitive foregut tube and associated organs, including liver and pancreas (Warga and Nusslein-Volhard 1999; Ober et al. 2004), indicating that the anterior endoderm undergoes morphogenetic events comparable to the movements of myocardial precursors. The molecular mechanisms that regulate this process, however, remain largely unexplored.

During vertebrate development, signaling initiated by ligands of the Wnt family instructs a wide array of cell behavior changes and morphogenetic events that contribute to specify, position, and shape a variety of organs, tissues, and structures (for review, see Peifer and Polakis 2000). In most of the instances characterized to date, Wnt ligands signal through the stabilization of β-catenin, via a specific intracellular signaling pathway

[1]Corresponding author.
E-MAIL belmonte@salk.edu; FAX (858) 453-2573.
Article and publication are at http://www.genesdev.org/cgi/doi/10.1101/gad.1253605.

known as the canonical Wnt pathway. More recently, several β-catenin-independent Wnt signaling pathways, known as noncanonical (nc), have been shown to be critical for different aspects of vertebrate embryo development, including convergence and extension (CE) movements during gastrulation and cardiogenesis (for review, see Veeman et al. 2003). Specifically, multiple genetic evidences underscore an important role of the nc-Wnt pathways in regulating CE movements during zebrafish embryo gastrulation. For example, mutations in zebrafish genes encoding Wnt ligands known to activate nc-Wnt pathways, such as *pipetail* (*ppt/wnt5*) and *silberblick* (*slb/wnt11*), result in defects in CE movements (Rauch et al. 1997; Heisenberg et al. 2000). In addition, mutations of *knypek* (*kny*) and *trilobite* (*tri*) genes (encoding two positive regulators of nc-Wnt signaling: a member of the glypican family of heparan sulfate proteoglycans and the transmembrane protein Strabismus/Van Gogh, respectively), result in stronger defects in CE movements than those of *ppt/wnt5* and *slb/wnt11* mutants (Topczewski et al. 2001; Jessen et al. 2002). Interestingly, *tri* mutants display additional phenotypic defects not present in *ppt/wnt5* and *slb/wnt11* mutants, such as defects in neuronal movements (Jessen et al. 2002), suggesting the possibility that partially redundant nc-Wnt signaling plays important roles during zebrafish embryo development, beyond the regulation of CE movements during gastrulation. This idea is also supported by the fact that components of the nc-Wnt signaling pathway are still expressed in late vertebrate embryos after gastrulation (Ungar et al. 1995; Topczewski et al. 2001).

Here, we use several strategies to investigate additional roles of the nc-Wnt signaling pathways beyond the control of CE movements during zebrafish embryo development and uncover a requirement of these pathways for the correct migration of heart and endodermal precursors toward the midline. Specifically, we identify *wnt4*, *slb/wnt11*, and *wnt11-related* (*wnt11r*) as the ligands that, by activating a nc-Wnt/Dishevelled/RhoA signaling pathway, regulate both CE movements and midline convergence of organ precursors. Furthermore, genetic and experimental evidence support the notion that defective endoderm morphogenesis is associated with defects in heart tube assembly. Our results reveal a novel regulatory mechanism, in which convergence of organ primordia to the midline requires a combined, redundant action of multiple Wnt ligands through the Dishevelled-RhoA branch of the nc-Wnt pathway.

Results

Noncanonical Wnt signaling controls midline convergence of heart primordia in zebrafish

Binding of specific Wnt ligands of the so-called Wnt5a-class to their cognate Frizzled receptors leads to activation of the multifunctional intracellular modular mediator Dishevelled (Dvl) (Wharton 2003). Dvl then can transduce the signal through a wide array of downstream effectors that include Ca^{2+}/CamKII, JNK, and the Rho GTPase family members RhoA, Rac1, and Cdc42 (Li et al. 1999; Habas et al. 2001, 2003; Sheldahl et al. 2003). Thus, an experimental strategy to inhibit the activities of nc-Wnt pathways is to block key intracellular signal transducers. In *Drosophila*, *Xenopus*, and mammalian cultured cells, a truncation mutant of Dvl (DvlΔDEP), which lacks the DEP domain, has been shown to act as a dominant-negative form of nc-Wnt signaling (Axelrod et al. 1998; Tada and Smith 2000; Wallingford et al. 2000; Habas et al. 2001). Thus, we decided to use DvlΔDEP to investigate the roles of nc-Wnt signaling in zebrafish development. To confirm that DvlΔDEP effectively inhibits nc-Wnt signaling in zebrafish embryos, we first tested the effect of injecting mRNA encoding DvlΔDEP into one-cell stage zebrafish embryos on the progression of CE movements during gastrulation, known to be controlled by nc-Wnt signaling (for review, see Veeman et al. 2003). Upon injection of 150 pg of DvlΔDEP mRNA, gastrulation defects were evident by 10 h post-fertilization (hpf), as has been reported for *slb/wnt11* mutants (Heisenberg et al. 2000). At this stage, the notochord of the injected embryos was short and wide, and the polster had not reached the anterior edge of the neural plate (Fig. 1B,B′). Transplantation experiments of FITC-labeled mesoendodermal cells clearly showed that CE movements were impaired in the embryos injected with 150 pg of DvlΔDEP (Fig. 1E,H), when compared to control embryos (Fig. 1D,G). These results indicate that DvlΔDEP inhibits nc-Wnt signaling in zebrafish embryos, as reported in other experimental systems (Axelrod et al. 1998; Tada and Smith 2000; Wallingford et al. 2000; Habas et al. 2001), and further confirm the requirements of Dvl-mediated nc-Wnt signaling for CE movements during zebrafish gastrulation. To investigate possible later roles of nc-Wnt signaling, we allowed embryos injected with 150 pg of DvlΔDEP to develop further, and observed multiple defects consistent with alterations in CE movements, including short anteroposterior (A/P) axis, microcephaly, and microphthalmia (Fig. 1K; see also Heisenberg et al. 2000). We also found additional developmental defects, the most obvious of these defects being the presence of pericardial edema and cardia bifida in about 50% of the embryos injected with 150 pg of DvlΔDEP (Fig. 1K,N; Table 1). Time-lapse imaging of myocardial migration clearly showed that cardia bifida phenotypes induced by DvlΔDEP injection result from the defective migration of myocardial precursors toward the midline (see below; Supplementary Movie 1B). Interestingly, injection of a lower amount of DvlΔDEP (30 pg) altered CE movements during gastrulation only slightly, as evaluated by the absence of gross morphological defects (Fig. 1C,L), or by the ability of transplanted FITC-labeled cells to correctly migrate during gastrulation ($n = 12$; Fig. 1F,I). Notably, a high percentage of embryos injected with 30 pg of DvlΔDEP displayed cardia bifida in the absence of noticeable alterations of the A/P axis (Fig. 1L,O; Table 1; Supplementary Movie 2). The fact that both actions could be separated by lowering the dose of injected DvlΔDEP argues strongly against cardia bifida

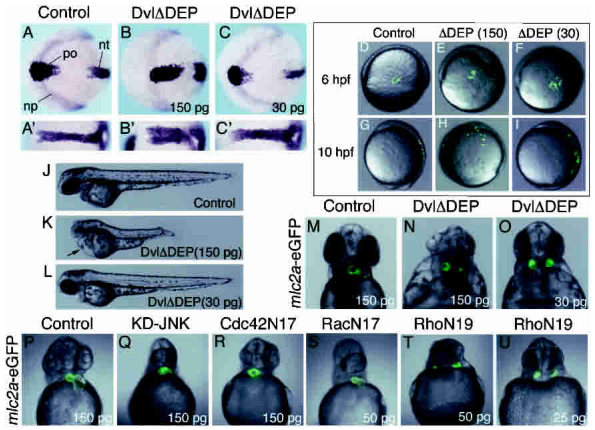

Figure 1. Early and late roles of noncanonical Wnt signaling in zebrafish embryos. (*A–I*) Inhibition of nc-Wnt signaling by DvlΔDEP affects CE movements. (*A–C*) *hgg1* (polster, po), *dlx3* (anterior edge of the neural plate, np), and *ntl* (developing notochord, nt) transcripts in 10 hpf embryos injected with 150 pg of mRNA encoding the negative control alkaline phosphatase (AP; Control, *A*), and 150 (*B*) or 30 (*C*) pg of mRNA encoding DvlΔDEP. Animal pole views, anterior to the left (*A–C*); dorsal view, anterior to the left (*A′–C′*). High concentrations of DvlΔDEP led to severe defects in CE movements, while lower concentration of DvlΔDEP altered CE only slightly. (*D–I*) Distribution of transplanted FITC-labeled cells at onset of gastrulation; lateral views, dorsal to the right. (*D,G*) Wild-type control. (*E,H*) DvlΔDEP (150 pg). (*F,I*) DvlΔDEP (30 pg). (*D–F*) Shield (6 hpf). (*G–I*) Tail bud (10 hpf). Dorsal convergence of mesoendodermal cells during zebrafish gastrulation was inhibited by high concentrations of DvlΔDEP (*E,H*), but not lower concentrations of DvlΔDEP (*F,I*). (*J–L*) Morphology of 48 hpf embryos injected with Control AP (*J*), DvlΔDEP (*K,L*), lateral views, anterior to the left. As consequences of CE defects, high doses of DvlΔDEP led to short A/P axis, microcephaly, and microphthalmia. In addition, DvlΔDEP injection induced pericardial edema (arrow in *K*). (*M–O*) Effects of DvlΔDEP on zebrafish heart development. Transgenic zebrafish embryos carrying *mlc2a*–eGFP reporter were injected with Control AP mRNA (*M*) or DvlΔDEP mRNA (*N,O*) and allowed to grow for 48 h. (*N,O*) Injection of DvlΔDEP even in low concentrations led to the formation of two laterally positioned hearts (cardia bifida) in zebrafish embryos. (*M–O*) Ventral views, anterior to the top. (*P–U*) Effect of downstream effectors of Dvl on heart tube assembly. *mlc2a*–eGFP transgenic zebrafish embryos were injected with mRNA encoding Control AP (150 pg) (*P*), KD-JNK (150 pg) (*Q*), Cdc42N17 (150 pg) (*R*), RacN17 (50 pg) (*S*), RhoN19 (25–50 pg) (*T,U*) and allowed to develop until 48 hpf. (*T,U*) Inhibition of Rho GTPase led to cardia bifida. Ventral views, anterior to the top.

being a defect secondary to alterations in CE movements during gastrulation. Rather, our data indicate that nc-Wnt signaling plays distinct, sequential roles for the control of CE movements and heart tube assembly, which require different thresholds of Dvl activity.

Noncanonical Wnt signaling controls midline convergence of heart primordia through Dvl-mediated activation of RhoA GTPase

A number of intracellular effectors have been shown to transduce Dvl-mediated nc-Wnt signaling including Ca^{2+}/PKC/CamKII, JNK, RhoA, Rac1, and Cdc42 pathways (for reviews, see Veeman et al. 2003; Wharton 2003). Therefore, we next investigated whether downregulation of any of these intracellular effectors could mimic the alterations induced by DvlΔDEP injection in the zebrafish embryo. Although varying degrees of morphological alterations compatible with altered CE movements (short A/P axis, microcephaly, and/or microphthalmia) were obtained in embryos injected with kinase-dead CamKII (KD-CamKII), kinase-dead JNK (KD-JNK), dominant-negative forms of Rac1 (RacN17), or Cdc42 (Cdc42N17), or treated with the PKC inhibitor bisindolylmalmeimide I, none of these treatments resulted in cardia bifida (Fig. 1P–S; Table 1), except for a small number of embryos injected with RacN17 (Table 1). Conversely, injection of a dominant-negative form of RhoA (RhoN19; Qiu et al. 1995) into zebrafish embryos caused alterations indistinguishable from those observed in embryos injected with DvlΔDEP, including a high frequency of cardia bifida (Fig. 1T,U; Table 1). Thus, injection of 50 pg of RhoN19 resulted in both CE defects and cardia bifida phenotypes (Fig. 1T; Table 1), whereas injection of lower amounts of RhoN19 (25 pg) resulted in cardia bifida in the absence of noticeable A/P axis defects (Fig. 1U; Table 1). These results indicate that RhoA GTPase, like Dvl, transduces signals that regulate both CE movements and heart tube assembly, and strongly suggest that the process of heart tube assembly is more sensitive than CE to experimental interference with Dvl/RhoA function.

We further verified the specificity of these loss-of-function studies with gain-of-function analyses. For this purpose, we analyzed the ability of constitutively active forms of the different Rho family GTPases to rescue the alterations induced by DvlΔDEP injection. Indeed, coinjection of DvlΔDEP with a constitutively active form of RhoA (RhoV14; Ridley and Hall 1992) prevented the appearance of cardia bifida in ~75% of injected embryos (13% vs. 50% cardia bifida in mock-rescue experiments), but could not rescue the defects in CE movements (Table 1). On the other hand, neither coinjection of active form of RacV12 nor Cdc42V12 with DvlΔDEP could rescue the cardia bifida phenotype or CE defects induced by DvlΔDEP (47% and 48%, respectively; Table 1). Our results so far indicate that Dvl-mediated nc-Wnt signaling regulates both CE movements and heart tube assembly through different downstream mediators of Dvl. Thus, CE movements during gastrulation are controlled by a wider subset of mediators of nc-Wnt signaling, including RhoA, Rac1, and Cdc42. In contrast, convergence of heart primordia about the midline is specifically regulated by Dvl-mediated activation of RhoA (hereafter referred to as nc-Wnt/Dvl/RhoA pathway).

Negative regulation of canonical Wnt/β-catenin signaling has been reported to be critical for proper heart development in chick and *Xenopus* embryos (Marvin et al. 2001; Schneider and Mercola 2001). It also has been reported that nc-Wnt signaling antagonizes the canonical Wnt/β-catenin signaling pathway in some experimental settings (Topol et al. 2003; Westfall et al. 2003).

Table 1. *Effects of interfering with intracellular mediators of Wnt signaling on heart tube assembly*

mRNA (pg)	*n*	Cardia bifida (%)	Other defects
Uninjected	1000	0	—
Alkaline phosphatase (150)	300	0.3	Abnormal body shape (1%)
DvlΔDEP (150)	420	49	Severe CE defects (99%)
DVlΔDEP (30)	400	23	Weak CE defects (5%)
KD-JNK (150)	122	1.6	CE defects (33%)
RhoN19 (50)	500	50	Severe CE defects (99%)
RhoN19 (25)	155	29	Weak CE defects (70%)
RacN17 (50)	196	5.1	Severe CE defects (93%)
Cdc42N17 (150)	141	0.9	CE defects (63%)
KD-CamKII (150)	158	0	Cyclopia, abnormal shape (20%)
Axin (150)	197	0.5	Short tail, small head (80%)
DvlΔDEP (150) + AP (10)	100	50	Severe CE defects (100%)
DvlΔDEP (150) + RhoV14 (10)	125	13[a]	Severe CE defects (100%)
DvlΔDEP (150) + RacV12 (10)	89	47	Severe CE defects (100%)
DvlΔDEP (150) + Cdc42V12 (10)	96	48	Severe CE defects (100%)

[a]Statistically significant (chi-square = 37.09; $p < 0.0001$) when compared to embryos injected with DvlΔDEP + Alkaline phosphatase (AP).

Therefore, it is possible that nc-Wnt signaling through Dvl/RhoA may somehow inhibit canonical Wnt/β-catenin signaling in heart tube assembly. To test this possibility, we injected mRNA encoding Axin, a known antagonist of β-catenin-dependent Wnt signaling (for review, see Peifer and Polakis 2000), into zebrafish embryos and analyzed its effects on heart tube assembly. We did not detect cardia bifida phenotypes in embryos injected with Axin in our experimental setting (Table 1), indicating that the function of nc-Wnt signaling in this process is unlikely to involve antagonism of canonical Wnt signaling.

wnt4a, slb/wnt11, *and* wnt11r *are expressed in mesoendoderm and midline structures during zebrafish heart morphogenesis*

Since down-regulation of nc-Wnt signaling with DvlΔDEP resulted in defects in midline convergence of heart primordia, and since this phenotype has not been described in zebrafish mutants of Wnt ligands that signal through Dvl-mediated nc-Wnt pathways, such as *slb* (Heisenberg et al. 2000) or *ppt* (Rauch et al. 1997), nor in double mutants of *slb/ppt* (Kilian et al. 2003), we reasoned that either the Wnt ligand involved in the process of midline convergence is not represented in the mutagenesis screens conducted so far or that several Wnt ligands act redundantly to regulate this process. To identify such a ligand(s), we undertook a search for Wnt-related genes expressed in zebrafish embryos during the relevant developmental window (14–18 hpf) by using a RT–PCR-based cloning approach (Gavin et al. 1990). We isolated several Wnt and Wnt-related genes including *wnt1* (Krauss et al. 1992), *wnt3a* (Buckles et al. 2004), *wnt4a* (Ungar et al. 1995), *ppt/wnt5* (Rauch et al. 1997), *wnt8b* (Kelly et al. 1995), *wnt10a* (Kelly et al. 1993), *slb/wnt11* (Heisenberg et al. 2000), and *wnt11r*, and selected those more likely to activate nc-Wnt signaling for further study. Analyses of the expression patterns of these candidates in zebrafish embryos from 12 to 24 hpf by in situ hybridization revealed that *ppt/wnt5* expression is restricted to the posterior mesoendoderm and tailbud (data not shown; see also Rauch et al. 1997; Kilian et al. 2003), while *wnt4a*, *slb/wnt11*, and *wnt11r* show spatial and temporal patterns of expression compatible with a role during heart tube assembly (Fig. 2). Thus, *wnt4a*, *slb/wnt11*, and *wnt11r* transcripts are expressed in neural ectoderm and mesoendoderm at 12 hpf (Fig. 2A,D,G,J,M,P; see also Ungar et al. 1995). After 12 hpf, *wnt4a* expression is restricted to the forebrain, floorplate, and neural tube, as well as to the anterior lateral plate mesoderm by 16 hpf (Fig. 2B,E). At 24 hpf, *wnt4a* transcripts appear mainly localized to neuroectoderm-derived structures (Fig. 2C,F). The expression of *slb/wnt11* overlaps with that of *wnt4a* in paraxial mesoendoderm at 12 hpf (Fig. 2, cf. J and D), although it becomes restricted to the notochord at 16 hpf (Fig. 2K) and to the developing somites and otic placodes at 24 hpf (Fig. 2I,L). The expression pattern of *wnt11r* overlaps that of *wnt4a* in the floorplate at 16 hpf and 24 hpf (Fig. 2, cf. N,O,Q,R and B,C,E,F), and with that of *slb/wnt11* in the developing somites at 24 hpf (Fig. 2, cf. R and L). Interestingly, *wnt11r* transcripts are also expressed in the heart tube at 24 hpf (Fig. 2O). These results indicate that the three Wnt ligands identified in our screen display expression patterns that partially overlap with each other, and suggest that their functions may be redundant.

wnt4a, slb/wnt11, *and* wnt11r *are all required for midline convergence of heart primordia*

To investigate the endogenous roles of *wnt4a*, *slb/wnt11*, and *wnt11r* during zebrafish embryo development, we knocked down their function by means of morpholino antisense oligonucleotides (MO). *slb/wnt11*-MO phenocopied the alterations in A/P axis and eye development

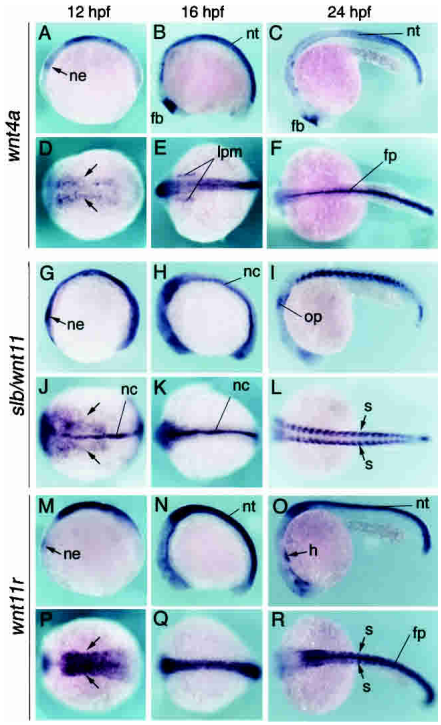

Figure 2. Spatial and temporal expression of *wnt4a*, *slb/wnt11*, and *wnt11r* during zebrafish heart morphogenesis. *wnt4a* (*A–F*), *slb/wnt11* (*G–L*), *wnt11r* (*M–R*) transcripts in zebrafish embryos at 12 hpf (*A,D,G,J,M,P*), 16 hpf (*B,E,H,K,N,Q*), and 24 hpf (*C,F,I,L,O,R*). Lateral (*A–C,G–I,M–O*) and dorsal (*D–F,J–K,P–R*) views, anterior to the left. Arrows in panels *D*, *J*, and *P* point at lateral edges of mesoendoderm. (ne) Neural ectoderm; (nt) neural tube; (fb) forebrain; (lpm) lateral plate mesoderm; (fp) floorplate; (nc) notochord; (op) otic placode; (s) somite; (h) heart.

present in *slb/wnt11* mutants (Table 2; Supplementary Fig. S1), which have been attributed to defects in CE movements during gastrulation (Heisenberg et al. 2000). Consistent with the weak expression of *wnt4a* and *wnt11r* during gastrulation (below the detection limits of in situ hybridization, but readily detectable by RT–PCR analysis; data not shown), both *wnt4a*-MO and *wnt11r*-MO, when injected separately, resulted in weak alterations in CE movements (Table 2; see also Supplementary Fig. S1), indicating that both *wnt4a* and *wnt11r* are required for proper control of CE movements. Despite inducing alterations in CE movements, knockdown of individual Wnt ligands (*wnt4a*, *slb/wnt11*, or *wnt11r*) did not result in defects in heart tube assembly (Table 2; Supplementary Fig. S1), indicating that none of the candidate Wnt ligands is solely responsible for controlling the migration of heart primordia toward the midline.

Therefore, we reasoned that the regulation of heart tube assembly by Wnt/Dvl/RhoA could be initiated by the redundant action of two or more of these Wnt ligands. To test this possibility, we injected combinations of MO against *wnt4a*, *slb/wnt11*, and *wnt11r*. Double knockdown experiments of *wnt4a* plus *wnt11r* or either *wnt4a* or *wnt11r* plus *slb/wnt11* typically resulted in CE defects much more severe than those induced by knockdown of individual Wnt ligands (Fig. 3A–D; see also Supplementary Fig. S1), confirming that *wnt4a*, *slb/wnt11*, and *wnt11r* play specific, nonredundant roles in the regulation of CE movements. Cardia bifida phenotypes were obtained in double knockdown experiments, but at extremely low frequencies (Table 2). In contrast, triple MO knockdown for *wnt4a*, *slb/wnt11*, and *wnt11r*, although not inducing significantly more severe CE defects (Fig. 3, cf. E and B–D), did result in a high incidence of cardia bifida phenotypes (almost one-third of injected embryos; Fig. 3O; Table 2). This confirms that a combined, redundant action of these three ligands controls the midline migration of heart primordia in zebrafish.

The specificity of alterations in heart tube assembly induced by combined knockdown of *wnt4a*, *slb/wnt11*, and *wnt11r* was assayed in rescue experiments using mRNA encoding each of the three ligands, a mutant form of Dvl that activates nc-Wnt signaling (DvlΔN; Habas et al. 2001), or constitutively active RhoA. All of these manipulations significantly reduced the frequency of cardia bifida phenotypes, while failing to rescue the CE defects (Table 2). Our results identify a branching of the nc-Wnt pathway, downstream of Dvl, that controls CE movements and heart tube assembly (see Discussion). Additionally, our results from MO experiments identify the Wnt ligands that control heart tube assembly, and uncover a combined, redundant role for *wnt4a*, *slb/wnt11*, and *wnt11r* to activate RhoA in this process.

Noncanonical Wnt/Dvl/RhoA is required for the migration of myocardial precursors, but not for their specification

Next, we investigated the cellular mechanisms responsible for the regulation of heart tube assembly by nc-Wnt/Dvl/RhoA signaling. Alterations in the convergence of heart primordia toward the midline have been found to depend on a failure of myocardial migration (for review, see Stainier 2001), defects in the specification of myocardial cell fate (Reiter et al. 1999; Yelon et al. 2000), the epithelial organization of the myocardial precursors (Trinh and Stainier 2004), or the differentiation of endoderm precursors (Schier et al. 1997; Alexander et al. 1999; Reiter et al. 1999; Kikuchi et al. 2000). Therefore, we began analyzing the dynamics of the defects in the migration of myocardial precursors caused by down-regulation of the Dvl/RhoA branch of the nc-Wnt pathway. For this purpose, we carried out time-lapse analyses of myocardial cell movements in control embryos or in embryos injected with DvlΔDEP or with dominant-negative RhoA. In control embryos, myocardial precursor cells were evidently bilateral at 14 hpf and progressively migrated toward the midline, where they formed a simple ring by 20 hpf ($n = 8$; Fig. 4A–C; Supplementary Movie 1A). However, myocardial precursors failed to migrate toward the midline in the embryos injected with either DvlΔDEP ($n = 16$; Fig. 4D–F; Supplementary Movie 1B) or dominant-negative RhoA ($n = 12$; data not shown), confirming that the Dvl/RhoA branch of the nc-Wnt pathway is required for myocardial migration to-

Table 2. *Summary of the effects of morpholino knockdowns of Wnt ligands on heart tube assembly*

Morpholino	*n*	Cardia bifida (%)	Other defects
Single MO experiments			
Control-MO	206	0.5	Short tail (15%)
wnt4a-MO	285	1.5	Weak CE defects (90%)
wnt4a(2)-MO	98	1.0	Weak CE defects (88%)
wnt11-MO	254	1.2	CE defects (99%)
wnt11r-MO	248	0.4	Weak CE defects (95%)
wnt11r(2)-MO	102	0.0	Weak CE defects (90%)
Double MO experiments			
wnt4a-MO + *wnt11*-MO	286	5.2	Severe CE defects (100%)
wnt4a-MO + *wnt11r*-MO	280	2.1	Severe CE defects (100%)
wnt11-MO + *wnt11r*-MO	233	1.2	Severe CE defects (100%)
Triple MO experiments			
wnt4a-MO + *wnt11*-MO + *wnt11r*-MO	212	30.1[a]	Severe CE defects (100%)
wnt4a-MO + *wnt11*-MO + *wnt11r*-MO + AP (100 pg)	90	33.3	Severe CE defects (100%)
wnt4a-MO + *wnt11*-MO + *wnt11r*-MO + RhoV14 (10 pg)	252	13.4[b]	Severe CE defects (100%)
wnt4a-MO + *wnt11*-MO + *wnt11r*-MO + DvlΔN (100 pg)	219	8.2[c]	Severe CE defects (100%)
wnt4a-MO + *wnt11*-MO + *wnt11r*-MO + *wnt4a* (100 pg)	168	17.8[d]	Severe CE defects (100%)
wnt4a-MO + *wnt11*-MO + *wnt11r*-MO + *wnt11* (100 pg)	164	8.5[e]	Severe CE defects (90%)
wnt4a-MO + *wnt11*-MO + *wnt11r*-MO + *wnt11r* (100 pg)	186	16.1[f]	Severe CE defects (95%)

We injected *wnt4a*-MO (3.0 ng), *wnt4a(2)*-MO (3.0 ng), *slb/wnt11*-MO (1.5 ng), *wnt11r*-MO (3.0 ng), and /or *wnt11r(2)*-MO (3.0 ng) in the indicated combinations into the one-cell stage of *mlc2a*-eGFP zebrafish embryos. The total amount of MO was adjusted to 7.5 ng with control-MO when necessary. *wnt4a(2)*-MO and *wnt11r(2)*-MO were also used in triple morpholino experiments, where both gave rise to significant cardia bifida phenotypes (8%–33%), depending on the specific combination tested.

[a]Statistically significant (chi-square = 53.95; $p < 0.0001$) when compared to embryos injected with control MO.

[b–f]Statistically significant [b](chi-square = 17.16; $p < 0.0005$), [c](chi-square = 30.66; $p < 0.0005$), [d](chi-square = 7.86; $p < 0.005$), [e](chi-square = 24.95; $p < 0.0005$), [f](chi-square = 10.55; $p < 0.005$), when compared to rescue induced by AP in triple morphants.

ward the midline, and that the defect in heart tube assembly results from the failure of the migration of these precursors.

To investigate whether the myocardial migration defects were a consequence of altered specification of myocardial precursors, we analyzed by in situ hybridization the expression levels of early and late markers of myocardial specification in embryos injected with DvlΔDEP, dominant-negative RhoA, or triple MOs against *wnt4a*, *slb/wnt11*, and *wnt11r*. Neither early (*nkx2.5*, *gata4*, or *faust/gata5*) nor late (*mlc2a*) markers of myocardial precursors displayed significant changes in the expression levels in embryos injected with DvlΔDEP (Fig. 4H,L; data not shown), dominant-negative RhoA (Fig. 4J,M; data not shown), or a combination of MO against *wnt4a*, *slb/wnt11*, and *wnt11r* (data not shown), even though heart primordia failed to fuse under these experimental conditions. These results indicate that specification of myocardial cell fate proceeds normally after down-regulation of the Dvl/RhoA branch of the nc-Wnt pathway.

Noncanonical Wnt/Dvl/RhoA signaling is required for the migration of endoderm precursors toward the midline

Since migration of myocardial precursors toward the midline has been proposed to depend on endoderm specification (for review, see Stainier 2001), we next investigated whether the defects in heart tube assembly induced by down-regulation of nc-Wnt/Dvl/RhoA signaling depended on endoderm specification. Unexpectedly, we found that expression of endoderm markers such as *gata4* and *faust/gata5* was detected bilaterally after down-regulation of Dvl/RhoA signaling (Fig. 4L,M; data not shown), as was the case for heart precursors. To gain further insights into the nature of endoderm alterations induced by down-regulation of Wnt/Dvl/RhoA signaling, we analyzed late points of endoderm morphogenesis by in situ hybridization for *foxA3* (general marker of endoderm derivatives), *ceruloplasmin* (*cp*) and *prox1* (markers of liver fate), and *insulin* and *pdx-1* (markers of pancreas differentiation) in 48 hpf control embryos or embryos injected with DvlΔDEP, dominant-negative RhoA, or a combination of MO against *wnt4a*, *slb/wnt11*, and *wnt11r* (Fig. 5; Supplementary Table S1). Either manipulation of the nc-Wnt pathway resulted in failure to fuse the anterior gut tube, giving rise to a Y-shaped tube (Fig. 5B,C; data not shown). Associated with this Y-shaped gut tube, liver and pancreas buds were formed bilaterally, indicating that the defects in midline convergence of endoderm affected foregut-derived structures rather than those of mid- or hindgut (Fig. 5E,F, H,I,N; data not shown). Furthermore, these defects could be rescued by coinjection of constitutively active RhoA with DvlΔDEP (20% vs. 56% in mock rescue experiments, $n = 120$ and 86, respectively). Thus, our data reveal that the Dvl/RhoA pathway activated by several Wnt ligands controls midline convergence of multiple organ primordia including the heart, gut, liver, and pancreas.

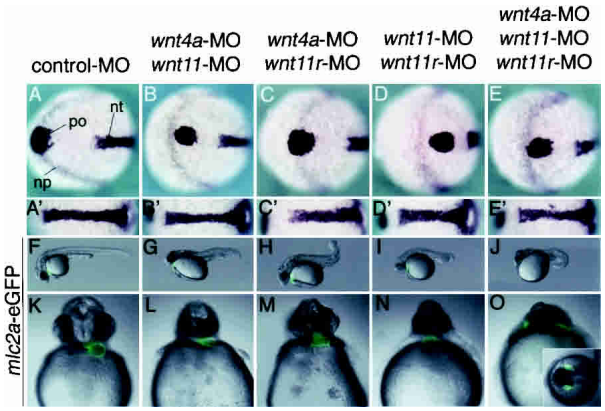

Figure 3. Combined, redundant action of *wnt4a*,*slb/wnt11*, and *wnt11r* is required for heart tube assembly. (*A–E*) *hgg1* (polster, po), *dlx3* (anterior edge of the neural plate, np), and *ntl* (developing notochord, nt) transcripts in 10 hpf zebrafish embryos injected with Control-MO (7.5 ng) (*A*), *wnt4a*-MO (3 ng) plus *slb/wnt11*-MO (1.5 ng) (*B*), *wnt4a*-MO (3 ng) plus *wnt11r*-MO (3 ng) (*C*), *slb/wnt11*-MO (1.5 ng) plus *wnt11r*-MO (3 ng) (*D*), or *wnt4a*-MO (3 ng) plus *slb/wnt11*-MO (1.5 ng) plus *wnt11r*-MO (3 ng) (*E*). Animal pole views, anterior to the left (*A–E*); dorsal view, anterior to the left (*A′–E′*). Double or triple knockdowns of wnt ligands led to similar defects of CE movements during gastrulation. (*F–O*) *mlc2a*–eGFP transgenic zebrafish embryos were injected with Control-MO (*F*,*K*), *wnt4a*-MO plus *slb/wnt11*-MO (*G*,*L*), *wnt4a*-MO plus *wnt11r*-MO (*H*,*M*), *slb/wnt11*-MO plus *wnt11r*-MO (*I*,*N*), or *wnt4a*-MO plus *slb/wnt11*-MO plus *wnt11r*-MO (*J*,*O*), and allowed to develop until 31 hpf. (*F–J*) Lateral views, anterior to the left. (*K–O*) Ventral views, anterior to the top. (*G*,*J*) Extensive areas of cell death were observed in double knockdown of *wnt4a* and *slb/wnt11* or triple knockdowns of *wnt4a*, *slb/wnt11*, and *wnt11r*. (*O*) Interestingly, only triple knockdowns of *wnt4a*, *slb/wnt11*, and *wnt11r* led to a significant occurence of cardia bifida. The *inset* in *O* shows cardia bifida caused by the triple knockdown (dorsal view, anterior to the left). See also Table 2.

Recently, a similar phenotype of failure to converge anterior endoderm structures was reported while studying the role of *vascular endothelial growth factor C* (*Vegfc*) in vascular development in the zebrafish (Ober et al. 2004). In this case, down-regulation of *Vegfc* function affected endoderm morphogenesis by reducing dorsal endoderm specification and by impairing foregut tube assembly. It is unlikely that the defect in anterior endoderm convergence is due to the defect in endoderm specification, for *squint* mutant embryos, in which formation of endoderm is also reduced, do not display alterations in foregut assembly (Ober et al. 2004). However, the fact that *Vegfc* down-regulation altered both processes does not allow for their clear separation. To investigate whether a defect in endoderm specification might be at the base of the foregut tube assembly defects induced by down-regulation of nc-Wnt/Dvl/RhoA signaling, we first analyzed the early steps of endoderm specification. In zebrafish embryos, *faust/gata5* is expressed before other endoderm markers such as *foxA2* or *gata4*, and is considered to be one of the earliest markers of endoderm fate determination (Reiter et al. 2001). Analyses of the expression of *gata5* in control and treated embryos at 9 hpf could not detect differences in either the levels of expression or the distribution of *gata5*-expressing cells (Fig. 5, cf. O and P), indicating that early endoderm specification is not altered after antagonism of the Dvl/RhoA pathway. Next, we investigated whether endodermal cells, though properly specified, displayed midline migration defects upon down-regulation of nc-Wnt/Dvl/RhoA signaling. In control embryos, *foxA2* is expressed by migrating endodermal cells, almost reaching the anterior midline by 16 hpf (Fig. 5Q); however, in embryos injected with either DvlΔDEP or dominant-negative RhoA, a high number of *foxA2*-positive anterior endoderm cells failed to coalesce in the midline (Fig. 5R). Similar results were obtained when analyzing the migration toward the midline of endoderm cells expressing *pdx-1* (Fig. 5T,V) or *nkx2.3* (marker of pharyngeal endoderm) (Lee et al. 1996; Fig. 5X). These results clearly indicate that anterior endoderm migration toward the midline, but not specification of endoderm precursors, is

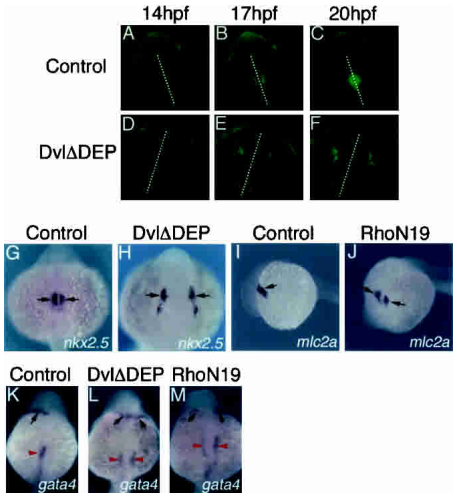

Figure 4. Noncanonical Wnt/Dvl/RhoA signaling regulates myocardial migration without affecting cell fate of myocardial precursors. (*A–F*) DvlΔDEP injection inhibits myocardial migration to the midline. Transgenic zebrafish embryos carrying a heart-specific *carp*–eGFP reporter were injected with AP (150 pg) or DvlΔDEP (150 pg) and allowed to develop until 13.5 hpf. Embryos were mounted into 1% agarose and time-lapse images of each embryo were obtained. Time-lapse images of control embryo (*A–C*) and DvlΔDEP-injected embryo (*D–F*) at 14 hpf (*A*,*D*), 17 hpf (*B*,*E*), and 20 hpf (*C*,*F*). White dotted lines indicate embryonic midline. Dorsal views, anterior to the top. (*D–F*) Myocardial precursor cells in DvlΔDEP-injected embryo failed to migrate to the midline. (*G–M*) *nkx2.5*, *mlc2a*, *gata4* transcripts in control (*G*,*I*,*K*) and DvlΔDEP-injected (*H*,*L*) or RhoN19-injected (*J*,*M*) embryos at 20 hpf (*G*,*H*) and 24 hpf (*I–M*). (*G*,*H*,*K–M*) Dorsal views, anterior to the top. (*I*,*J*) Lateral views, anterior to the left. *nkx2.5*- *mlc2a*- or *gata4*-expressing myocardial precursors (black arrows) were distributed bilaterally in DvlΔDEP-injected (*H*,*L*) or RhoN19-injected (*J*,*M*) embryos, but the levels of expression were not changed as compared to those of Control (*G*,*I*,*K*). Note: *gata4* is also expressed in endoderm. In DvlΔDEP-injected (*L*) or RhoN19-injected (*M*) embryos, *gata4*-expressing endodermal domains were duplicated (red arrows).

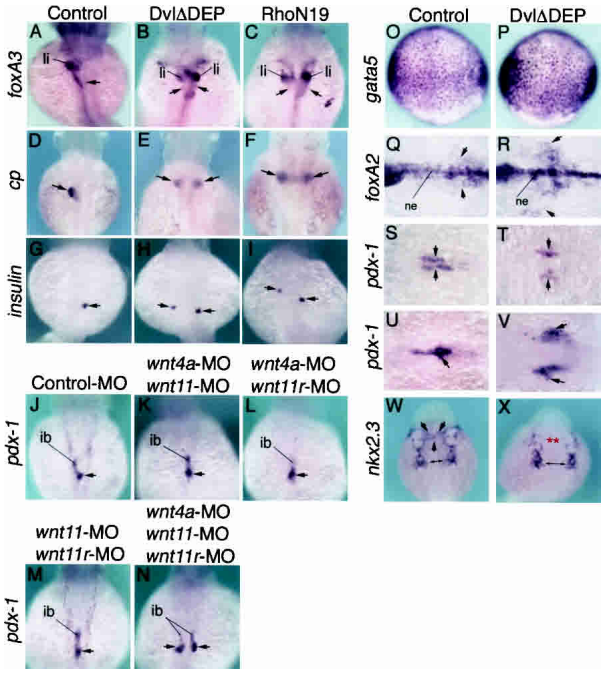

Figure 5. Noncanonical Wnt/Dvl/RhoA signaling regulates midline convergence of foregut endoderm precursors without affecting their cell fate. (*A–I*) *foxA3* (*A–C*), *ceruloplasmin* (*cp*) (*D–F*), and *insulin* (*G–I*) transcripts in 48 hpf embryos injected with Control AP (*A*,*D*,*G*), DvlΔDEP (*B*,*E*,*H*), or RhoN19 (*C*,*F*,*I*); dorsal views, anterior to the top. Antagonizing nc-Wnt signaling led to the formation of a Y-shaped gut tube (*B*,*C*), and the duplication of liver (*E*,*F*) and pancreas (*H*,*I*) buds. (li) liver buds. (*J–N*) *pdx-1* expression in 42 hpf embryos injected with Control-MO (*J*), *wnt4a*-MO plus *slb/wnt11*-MO (*K*), *wnt4a*-MO plus *wnt11r*-MO (*L*), *slb/wnt11*-MO plus *wnt11r*-MO (*M*), or *wnt4a*-MO plus *slb/wnt11*-MO plus *wnt11r*-MO (*N*); dorsal views, anterior to the top. Arrows indicate *pdx-1*-expressing pancreas bud. (ib) intestinal bulb. Only triple knockdown experiments of *wnt4*, *slb/wnt11*, and *wnt11r* resulted in the duplication of pancreas and intestinal bulbs (*N*). (*O–X*) Expression of *gata5* (*O*,*P*), *foxA2* (*Q*,*R*), *pdx-1* (*S–V*), and *nkx2.3* (*W*,*X*) in Control (*O*,*Q*, *S*,*U*,*W*) and DvlΔDEP-injected (*P*,*R*,*T*,*V*,*X*) embryos. (*O*,*P*) Ninety percent epiboly (9 hpf), dorsal views, anterior to the top. Expression levels of *gata5* in endodermal precursors were not changed in DvlΔDEP-injected (*P*) embryos as compared with that of Control (*O*). (*Q*,*R*) Sixteen hours post-fertilization, dorsal views, anterior to the left. *foxA2* is expressed in anterior endoderm and ventral neuroectoderm (ne) along the midline. (*R*) In DvlΔDEP-injected embryos, a large number of *foxA2*-expressing endodermal cells (arrows) failed to coalesce in the midline. (*S–V*) Pancreas primordia marked by *pdx-1* did not coalesce in the midline in embryos injected with DvlΔDEP (*T*,*V*). (*S*,*T*) Sixteen hours post-fertilization. (*U*,*V*) Twenty-four hours post-fertilization. Dorsal views, anterior to the left. (*W*,*X*) In DvlΔDEP-injected embryos, posterior *nkx2.3*-expressing pharyngeal endoderm (double arrows in *X*) appeared wider along the mediolateral axis, as compared to control (*W*). Most anterior *nkx2.3*-expressing pharyngeal endodermal cells (black arrows in *W*) failed to migrate toward the midline in DvlΔDEP-injected embryos (red asterisks).

defective in embryos in which nc-Wnt/Dvl/RhoA signaling has been inhibited. Together with our results from myocardial migration analyses, our data uncover a mechanism by which nc-Wnt signaling, intracellularly transduced by the RhoA branch of Dvl-mediated signaling pathways, controls the convergence toward the midline of both endoderm- and mesoderm-derived organ primordia, without affecting the specification of progenitors for either structure. When put in the context of additional evidence from genetic zebrafish mutants, we propose that the general control of organ primordia morphogenesis by nc-Wnt signaling is most likely to be directly regulated at the level of endoderm migration (see Discussion).

Discussion

Many unpaired organs of the vertebrate body plan, such as the heart, gut tube, liver, and pancreas, develop as bilateral primordia that later during embryogenesis migrate and fuse about the embryo midline. Here we show that, in the zebrafish, this process is regulated by multiple redundant Wnt ligands that signal through noncanonical (β-catenin-independent) pathways.

The Dvl/RhoA branch of noncanonical Wnt signaling regulates midline convergence of myocardial precursors

In zebrafish and *Xenopus* embryos, several components of the nc-Wnt signaling pathway have been implicated in CE movements during gastrulation (for reviews, see Wallingford et al. 2002; Veeman et al. 2003). In this study, we further confirm the requirements of several intracellular mediators of nc-Wnt signaling, including RhoA, Rac1, Cdc42, and JNK, for CE movements in zebrafish embryos (Fig. 1; Table 1; see also Bakkers et al. 2004), consistent with results from *Xenopus* (Habas et al. 2001, 2003; Yamanaka et al. 2002). Our results also identify *wnt4a* and *wnt11r* as novel regulators of CE movements (Fig. 3; Table 2; see Supplementary Fig. S1). Interestingly, combined down-regulation of *wnt4a* and *wnt11r*, or of either *wnt4a* or *wnt11r* and *slb/wnt11*, results in stronger CE defects than those elicited by manipulation of individual ligands (Fig. 3; see Supplementary Fig. S1), indicating the existence of nonredundant regulatory roles of multiple nc-Wnt signaling pathways for the initiation and/or progression of CE movements during gastrulation. In contrast to the regulation of CE movements, we find a combined, redundant action of three Wnt ligands (*wnt4a*, *slb/wnt11*, and *wnt11r*) on midline convergence of organ precursors through the Dvl/RhoA branch of nc-Wnt signaling. Thus, relatively low levels of constitutively active RhoA efficiently rescues defects in midline convergence of organ precursors, but not the defects in CE movements, induced by injection of DvlΔDEP or of a combination of MO against *wnt4a*, *slb/wnt11*, and *wnt11r* (Tables 1, 2). These results reveal a splitting of the nc-Wnt pathway downstream of Dvl; the Dvl/RhoA branch of this pathway is critically required for the control of midline convergence (which appears to be very sensitive to interference with

Dvl/RhoA activity), whereas a wider subset of mediators downstream of Dvl appears to mediate the control of CE movements.

Since our results demonstrate that nc-Wnt signaling regulates both CE movements and midline convergence of organ precursors in the zebrafish embryos, it is formally possible that the alterations in the midline convergence induced by down-regulation of nc-Wnt/Dvl/RhoA signaling were secondary to earlier defects in CE movements. Two main lines of evidence argue against this possibility: (1) Down-regulation of noncanonical Wnt signaling in *ppt/wnt5*, *slb/wnt11*, *kny*, or *tri* mutants, in crosses among them (Rauch et al. 1997; Heisenberg et al. 2000; Topczewski et al. 2001; Jessen et al. 2002), or by knocking down *ppt/wnt5* (Lele et al. 2001), *slb/wnt11* (Lele et al. 2001; this report), *wnt4a*, or *wnt11r* (this report), result in varying degrees of defects in CE movements, but are not associated with alterations of heart tube assembly. (2) Conversely, injection of low doses of DvlΔDEP or dominant-negative RhoA induce cardia bifida in the absence of significant alterations in CE movements during gastrulation (Fig. 1).

Furthermore, our data in the zebrafish uncover an evolutionarily conserved regulatory mechanism consistent with the fact that inhibition of Rho kinases (downstream effectors of RhoA) in whole-embryo culture in chick and mouse leads to a cardia bifida phenotype (Wei et al. 2001). Taken together, our results in the zebrafish are consistent with a general role of noncanonical Wnt signaling controlling cell behavior, rather than cell fate (Veeman et al. 2003).

Noncanonical Wnt/Dvl/RhoA signaling controls foregut tube assembly

As was the case for heart tube assembly, our results demonstrate that nc-Wnt/Dvl/RhoA signaling specifically regulates endoderm migration toward the midline without affecting cell fate determination. Thus, our results provide an entry point to analyze the phenomenon of foregut tube assembly. Indeed, understanding the molecular and cellular mechanisms of foregut assembly has far-reaching implications that extend to human disease. For instance, the incidence of *pancreas divisum* in the general population is estimated between 5% and 10%, the vast majority of cases being of type I, or total failure of fusion (Quest and Lombard 2000). Less prevalent are a number of congenital malformations collectively known as alimentary tract duplications, with an estimated prevalence of 1:4,500 (Michalsky and Besner 2004). Typically, these alterations are diagnosed in early infancy and require extensive surgery, with an associated mortality around 10% (Carachi and Azmy 2002). Unfortunately, the absence of suitable animal models for these developmental alterations has contributed to our lack of knowledge about their pathogenesis, which remains obscure (Michalsky and Besner 2004). The possibility of experimentally manipulating the convergence of anterior endoderm in the zebrafish embryo provides new tools for understanding how this process is regulated during normal development, and how some of these congenital alterations may occur. In this respect, our data uncover a key regulatory mechanism for this process that may be of relevance for diagnostic and/or therapeutic applications.

From a basic research viewpoint, our results also provide novel insights into the relationships between endoderm and heart morphogenesis. It has been proposed that myocardial morphogenesis and endoderm specification are intimately related and, according to a long-held view, mechanistically linked (for review, see Stainier 2001). This hypothesis is supported by the existence of myocardial migration defects in a variety of zebrafish mutants with impaired endoderm formation (Schier et al. 1997; Alexander et al. 1999; Reiter et al. 1999; Kikuchi et al. 2000), by experimental results in the chick embryo, where surgical removal of anterior endoderm leads to failure of heart tube assembly (Withington et al. 2001), and by the fact that some alterations in heart tube assembly can be rescued by transplantation of wild-type endodermal cells into mutant zebrafish (David and Rosa 2001) or mouse embryos (Narita et al. 1997). It is debatable, however, whether the endoderm acts as a substrate for myocardial migration, it provides an instructive signal for heart tube assembly, or both.

In this respect, our studies are particularly helpful, inasmuch as we identify a novel regulatory mechanism of heart and foregut tube assembly by nc-Wnt signaling that depends on neither myocardial nor endoderm specification. Together with previous analyses of zebrafish mutants that lack endoderm (Schier et al. 1997; Alexander et al. 1999; Reiter et al. 1999; Kikuchi et al. 2000), our results provide strong support for a scenario in which heart tube assembly requires the presence of a contacting layer of anterior endoderm at the midline, and suggest that the primary role of nc-Wnt/Dvl/RhoA signaling in this process is the control of anterior endoderm migration. This scenario is supported by several lines of evidence: (1) Heart tube assembly does not occur in mutants with absolute absence of endoderm (Schier et al. 1997; Alexander et al. 1999; Reiter et al. 1999; Kikuchi et al. 2000; see also Supplementary Fig. S2). (2) The migration of anterior endoderm precursors does not depend on heart tube assembly, since *miles apart* mutant embryos (Kupperman et al. 2000), which display cardia bifida, show normal anterior endoderm morphogenesis (Supplementary Fig. S2). (3) In control zebrafish embryos, the migration of endoderm precursors toward the midline precedes that of heart primordia (cf. Figs. 5Q and 4A–C,G). (4) After down-regulation of nc-Wnt/Dvl/RhoA signaling, the failure in midline convergence of endoderm precursors precedes the defect in myocardial migration and is restricted to the anterior domain (Fig. 5T,V,X). (5) Both defects are highly correlated after our experimental manipulations of nc-Wnt/Dvl/RhoA signaling (95%, $n = 86$, and 94%, $n = 70$, of cardia bifida phenotypes are associated to failure of anterior endoderm convergence in embryos injected with DvlΔDEP or RhoN19, respectively). (6) The alterations in endoderm migration in-

duced by down-regulation of *Vegfc* function (Ober et al. 2004) are frequently associated with a cardia bifida phenotype (E. Ober and D.Y.R. Stainier, pers. commun.).

In this study, we demonstrate that nc-Wnt signaling regulates complex cell migration events that determine not only the initial layout of the three embryonic germ layers during gastrulation, but also specific morphogenetic processes such as the midline migration of heart and foregut precursors. We show that regulation of endoderm morphogenesis depends on redundant activation of nc-Wnt signaling transduced by the small GTPase RhoA. These results allowed us to provide new insights into the mechanistic relationships of endoderm and myocardial morphogenesis. Similarly, a detailed dissection of the requirements of different nc-Wnt pathways for CE movements during gastrulation will undoubtedly further our understanding of earlier steps of vertebrate embryo development.

Materials and methods

Fish lines and whole-mount in situ hybridization

Wild-type (AB), *mlc2a*–eGFP (Raya et al. 2003), *carp*–eGFP (Raya et al. 2003), *oep*::*mlc2a*–eGFP [*tz257*/+::*mlc2a/mlc2a*], *mil*::*mlc2a*–eGFP [*te273*/+::*mlc2a/mlc2a*] were used for this work. Whole-mount in situ hybridization was performed as described (Ng et al. 2002). The cDNA fragments for *distal-less 3* (*dlx3*), *hatching gland 1* (*hgg1*), *no tail* (*ntl*), *nkx2.3*, *nkx2.5*, *mlc2a*, *gata4*, *gata5*, *foxA2*, *foxA3*, *ceruloplasmin* (*cp*), *prox1*, *insulin*, and *pdx-1* were utilized for the antisense probes.

Constructs, morpholinos, and injection

pCS2+ vectors carrying cDNA fragments encoding alkaline phosphatase (AP), DvlΔDEP, Axin, Kinase dead-CamKII (K42M) RhoN19, RhoV14, RacN17, RacV12, Cdc42N17, Cdc42V12, and kinase dead-JNK (T183A, Y185F) were used in this study. mRNAs were synthesized using the SP6 mMessage mMachine System (Ambion). Capped mRNAs were injected into one-cell stage embryos as described (Ng et al. 2002).

Morpholinos

Antisense morpholino oligonucleotides against *wnt4a*, *wnt11*, and *wnt11r* were designed to inhibit RNA translation, and were obtained from Gene Tools. The sequences were as follows: Control-MO, 5′-CCTCTTACCTCAGTTACAATTTATA-3′; *wnt4*-MO, 5′-CTCCGATGACATCTTTAGTGGAATC-3′; *wnt4(2)*-MO, 5′-AGCTAAGTAAAGGTTGCTGGTGTAA-3′ *wnt11*-MO, 5′-GTTCCTGTATTCTGTCATGTCGCTC-3′; *wnt11r*-MO, 5′-AGGGAAGGTTCGCTTCATGCTGTAC-3′; and *wnt11r(2)*-MO, 5′-AAGATCCAGAAGACACTGATGCAGG-3′.

The efficacy of all MOs was tested in vivo by coinjecting mRNA encoding their cognate Wnt–eGFP fusion protein (Supplementary Fig. S1).

Cell transplantations

Donor embryos were injected with FITC-dextran along with control AP or DvlΔDEP mRNA. At the shield stage, 10–20 donor mesoendodermal cells at the lateral marginal zone were transplanted into the same region of the same type of recipient embryos. Chimeric embryos were mounted into 1.5% methylcellulose, and pictures were taken at shield stage and bud stage with a Zeiss Stemi SV11 Apo microscope and OPENLAB software.

Cloning of zebrafish wnt *genes*

PCR amplification was performed using degenerate primers as described previously (Gavin et al. 1990), using polyA-tailed cDNA of 14–18 hpf zebrafish embryos as template. The amplified PCR fragments were cloned into pCR-II (Invitrogen), and their sequences verified by nucleotide sequencing. We identified eight different Wnt-related genes from their sequence information.

Time-lapse imaging

carp–eGFP transgenic zebrafish embryos were injected with AP, DvlΔDEP, or RhoN19 RNA and were allowed to develop until 14 hpf. These embryos were mounted into 1% low-melt agarose. Time-lapse image acquisition was performed with a Leica DMIRE2 microscope and OPENLAB software.

Acknowledgments

We are grateful to Elke A. Ober and Didier Y.R. Stainier for sharing unpublished information, helpful discussions, and reagents. We also thank May Schwarz for help in preparing the manuscript; Ilir Dubova, Marina Raya, and Gabriel Sternik for their technical assistance; Tohru Itoh, Augustus Lestick, Masanobu Morita, Isao Oishi, and Atsushi Suzuki for helpful discussions; and Raymond Habas, Xi He, Atsushi Miyajima, Randall T. Moon, Takaya Sato, Alex Schier, Masazumi Tada, and Kristiina Vuori for reagents. T.M. is supported by a JSPS postdoctoral fellowship for Research Abroad, Japan. A.R. and C.R.E. are partially supported by a postdoctoral fellowship from Fundación Inbiomed, Spain. This work was supported by grants from the American Heart Association, the NIH, and the G. Harold and Leila Y. Mathers Charitable Foundation to J.C.I.B.

References

Alexander, J., Rothenberg, M., Henry, G.L., and Stainier, D.Y. 1999. casanova plays an early and essential role in endoderm formation in zebrafish. *Dev. Biol.* **215:** 343–357.

Axelrod, J.D., Miller, J.R., Shulman, J.M., Moon, R.T., and Perrimon, N. 1998. Differential recruitment of Dishevelled provides signaling specificity in the planar cell polarity and Wingless signaling pathways. *Genes & Dev.* **12:** 2610–2622.

Bakkers, J., Kramer, C., Pothof, J., Quaedvlieg, N.E., Spaink, H.P., and Hammerschmidt, M. 2004. Has2 is required upstream of Rac1 to govern dorsal migration of lateral cells during zebrafish gastrulation. *Development* **131:** 525–537.

Buckles, G.R., Thorpe, C.J., Ramel, M.C., and Lekven, A.C. 2004. Combinatorial Wnt control of zebrafish midbrain–hindbrain boundary formation. *Mech. Dev.* **121:** 437–447.

Carachi, R. and Azmy, A. 2002. Foregut duplications. *Pediatr. Surg. Int.* **18:** 371–374.

Chen, J.N., Haffter, P., Odenthal, J., Vogelsang, E., Brand, M., van Eeden, F.J., Furutani-Seiki, M., Granato, M., Hammerschmidt, M., Heisenberg, C.P., et al. 1996. Mutations affecting the cardiovascular system and other internal organs in zebrafish. *Development* **123:** 293–302.

David, N.B. and Rosa, F.M. 2001. Cell autonomous commit-

ment to an endodermal fate and behaviour by activation of Nodal signalling. *Development* **128:** 3937–3947.
Gavin, B.J., McMahon, J.A., and McMahon, A.P. 1990. Expression of multiple novel Wnt-1/int-1-related genes during fetal and adult mouse development. *Genes & Dev.* **4:** 2319–2332.
Habas, R., Kato, Y., and He, X. 2001. Wnt/Frizzled activation of Rho regulates vertebrate gastrulation and requires a novel Formin homology protein Daam1. *Cell* **107:** 843–854.
Habas, R., Dawid, I.B., and He, X. 2003. Coactivation of Rac and Rho by Wnt/Frizzled signaling is required for vertebrate gastrulation. *Genes & Dev.* **17:** 295–309.
Heisenberg, C.P., Tada, M., Rauch, G.J., Saude, L., Concha, M.L., Geisler, R., Stemple, D.L., Smith, J.C., and Wilson, S.W. 2000. Silberblick/Wnt11 mediates convergent extension movements during zebrafish gastrulation. *Nature* **405:** 76–81.
Jessen, J.R., Topczewski, J., Bingham, S., Sepich, D.S., Marlow, F., Chandrasekhar, A., and Solnica-Krezel, L. 2002. Zebrafish trilobite identifies new roles for Strabismus in gastrulation and neuronal movements. *Nat. Cell Biol.* **4:** 610–615.
Kelly, G.M., Lai, C.J., and Moon, R.T. 1993. Expression of wnt10a in the central nervous system of developing zebrafish. *Dev. Biol.* **158:** 113–121.
Kelly, G.M., Greenstein, P., Erezyilmaz, D.F., and Moon, R.T. 1995. Zebrafish wnt8 and wnt8b share a common activity but are involved in distinct developmental pathways. *Development* **121:** 1787–1799.
Kikuchi, Y., Trinh, L.A., Reiter, J.F., Alexander, J., Yelon, D., and Stainier, D.Y. 2000. The zebrafish bonnie and clyde gene encodes a Mix family homeodomain protein that regulates the generation of endodermal precursors. *Genes & Dev.* **14:** 1279–1289.
Kilian, B., Mansukoski, H., Barbosa, F.C., Ulrich, F., Tada, M., and Heisenberg, C.P. 2003. The role of Ppt/Wnt5 in regulating cell shape and movement during zebrafish gastrulation. *Mech. Dev.* **120:** 467–476.
Krauss, S., Korzh, V., Fjose, A., and Johansen, T. 1992. Expression of four zebrafish wnt-related genes during embryogenesis. *Development* **116:** 249–259.
Kupperman, E., An, S., Osborne, N., Waldron, S., and Stainier, D.Y. 2000. A sphingosine-1-phosphate receptor regulates cell migration during vertebrate heart development. *Nature* **406:** 192–195.
Lee, K.H., Xu, Q., and Breitbart, R.E. 1996. A new tinman-related gene, nkx2.7, anticipates the expression of nkx2.5 and nkx2.3 in zebrafish heart and pharyngeal endoderm. *Dev. Biol.* **180:** 722–731.
Lele, Z., Bakkers, J., and Hammerschmidt, M. 2001. Morpholino phenocopies of the swirl, snailhouse, somitabun, minifin, silberblick, and pipetail mutations. *Genesis* **30:** 190–194.
Li, L., Yuan, H., Xie, W., Mao, J., Caruso, A.M., McMahon, A., Sussman, D.J., and Wu, D. 1999. Dishevelled proteins lead to two signaling pathways. Regulation of LEF-1 and c-Jun N-terminal kinase in mammalian cells. *J. Biol. Chem.* **274:** 129–134.
Marvin, M.J., Di Rocco, G., Gardiner, A., Bush, S.M., and Lassar, A.B. 2001. Inhibition of Wnt activity induces heart formation from posterior mesoderm. *Genes & Dev.* **15:** 316–327.
Michalsky, M. and Besner, G.E. 2004. Alimentary tract duplications. *eMedicine J.* **5:** http://author.emedicine.com/PED/topic2922.htm.
Narita, N., Bielinska, M., and Wilson, D.B. 1997. Wild-type endoderm abrogates the ventral developmental defects associated with GATA-4 deficiency in the mouse. *Dev. Biol.* **189:** 270–274.
Ng, J.K., Kawakami, Y., Buscher, D., Raya, A., Itoh, T., Koth, C.M., Rodriguez Esteban, C., Rodriguez-Leon, J., Garrity, D.M., Fishman, M.C., et al. 2002. The limb identity gene Tbx5 promotes limb initiation by interacting with Wnt2b and Fgf10. *Development* **129:** 5161–5170.
Ober, E.A., Olofsson, B., Makinen, T., Jin, S.W., Shoji, W., Koh, G.Y., Alitalo, K., and Stainier, D.Y. 2004. Vegfc is required for vascular development and endoderm morphogenesis in zebrafish. *EMBO Rep.* **5:** 78–84.
Peifer, M. and Polakis, P. 2000. Wnt signaling in oncogenesis and embryogenesis—A look outside the nucleus. *Science* **287:** 1606–1609.
Qiu, R.G., Chen, J., McCormick, F., and Symons, M. 1995. A role for Rho in Ras transformation. *Proc. Natl. Acad. Sci.* **92:** 11781–11785.
Quest, L. and Lombard, M. 2000. Pancreas divisum: Opinio divisa. *Gut* **47:** 317–319.
Rauch, G.J., Hammerschmidt, M., Blader, P., Schauerte, H.E., Strahle, U., Ingham, P.W., McMahon, A.P., and Haffter, P. 1997. Wnt5 is required for tail formation in the zebrafish embryo. *Cold Spring Harb. Symp. Quant. Biol.* **62:** 227–234.
Raya, A., Koth, C.M., Buscher, D., Kawakami, Y., Itoh, T., Raya, R.M., Sternik, G., Tsai, H.J., Rodriguez-Esteban, C., and Izpisua-Belmonte, J.C. 2003. Activation of Notch signaling pathway precedes heart regeneration in zebrafish. *Proc. Natl. Acad. Sci.* **100(Suppl. 1):** 11889–11895.
Reiter, J.F., Alexander, J., Rodaway, A., Yelon, D., Patient, R., Holder, N., and Stainier, D.Y. 1999. Gata5 is required for the development of the heart and endoderm in zebrafish. *Genes & Dev.* **13:** 2983–2995.
Reiter, J.F., Kikuchi, Y., and Stainier, D.Y. 2001. Multiple roles for Gata5 in zebrafish endoderm formation. *Development* **128:** 125–135.
Ridley, A.J. and Hall, A. 1992. The small GTP-binding protein rho regulates the assembly of focal adhesions and actin stress fibers in response to growth factors. *Cell* **70:** 389–399.
Schier, A.F., Neuhauss, S.C., Helde, K.A., Talbot, W.S., and Driever, W. 1997. The one-eyed pinhead gene functions in mesoderm and endoderm formation in zebrafish and interacts with no tail. *Development* **124:** 327–342.
Schneider, V.A. and Mercola, M. 2001. Wnt antagonism initiates cardiogenesis in *Xenopus laevis*. *Genes & Dev.* **15:** 304–315.
Sheldahl, L.C., Slusarski, D.C., Pandur, P., Miller, J.R., Kuhl, M., and Moon, R.T. 2003. Dishevelled activates Ca^{2+} flux, PKC, and CamKII in vertebrate embryos. *J. Cell Biol.* **161:** 769–77.
Stainier, D.Y. 2001. Zebrafish genetics and vertebrate heart formation. *Nat. Rev. Genet.* **2:** 39–48.
Stainier, D.Y., Fouquet, B., Chen, J.N., Warren, K.S., Weinstein, B.M., Meiler, S.E., Mohideen, M.A., Neuhauss, S.C., Solnica-Krezel, L., Schier, A.F., et al. 1996. Mutations affecting the formation and function of the cardiovascular system in the zebrafish embryo. *Development* **123:** 285–292.
Tada, M. and Smith, J.C. 2000. Xwnt11 is a target of *Xenopus* Brachyury: Regulation of gastrulation movements via Dishevelled, but not through the canonical Wnt pathway. *Development* **127:** 2227–2238.
Topczewski, J., Sepich, D.S., Myers, D.C., Walker, C., Amores, A., Lele, Z., Hammerschmidt, M., Postlethwait, J., and Solnica-Krezel, L. 2001. The zebrafish glypican knypek controls cell polarity during gastrulation movements of convergent extension. *Dev. Cell* **1:** 251–264.
Topol, L., Jiang, X., Choi, H., Garrett-Beal, L., Carolan, P.J., and Yang, Y. 2003. Wnt-5a inhibits the canonical Wnt pathway by promoting GSK-3-independent beta-catenin degradation.

J. Cell. Biol. **162:** 899–908.
Trinh, L.A. and Stainier, D.Y. 2004. Fibronectin regulates epithelial organization during myocardial migration in zebrafish. *Dev. Cell* **6:** 371–382.
Ungar, A.R., Kelly, G.M., and Moon, R.T. 1995. Wnt4 affects morphogenesis when misexpressed in the zebrafish embryo. *Mech. Dev.* **52:** 153–164.
Veeman, M.T., Axelrod, J.D., and Moon, R.T. 2003. A second canon. Functions and mechanisms of beta-catenin-independent Wnt signaling. *Dev. Cell* **5:** 367–377.
Wallingford, J.B., Rowning, B.A., Vogeli, K.M., Rothbacher, U., Fraser, S.E., and Harland, R.M. 2000. Dishevelled controls cell polarity during *Xenopus* gastrulation. *Nature* **405:** 81–85.
Wallingford, J.B., Fraser, S.E., and Harland, R.M. 2002. Convergent extension: The molecular control of polarized cell movement during embryonic development. *Dev. Cell* **2:** 695–706.
Warga, R.M. and Nusslein-Volhard, C. 1999. Origin and development of the zebrafish endoderm. *Development* **126:** 827–838.
Wei, L., Roberts, W., Wang, L., Yamada, M., Zhang, S., Zhao, Z., Rivkees, S.A., Schwartz, R.J., and Imanaka-Yoshida, K. 2001. Rho kinases play an obligatory role in vertebrate embryonic organogenesis. *Development* **128:** 2953–2962.
Westfall, T.A., Brimeyer, R., Twedt, J., Gladon, J., Olberding, A., Furutani-Seiki, M., and Slusarski, D.C. 2003. Wnt-5/pipetail functions in vertebrate axis formation as a negative regulator of Wnt/beta-catenin activity. *J. Cell Biol.* **162:** 889–898.
Wharton Jr., K.A. 2003. Runnin' with the Dvl: Proteins that associate with Dsh/Dvl and their significance to Wnt signal transduction. *Dev. Biol.* **253:** 1–17.
Withington, S., Beddington, R., and Cooke, J. 2001. Foregut endoderm is required at head process stages for anteriormost neural patterning in chick. *Development* **128:** 309–320.
Yamanaka, H., Moriguchi, T., Masuyama, N., Kusakabe, M., Hanafusa, H., Takada, R., Takada, S., and Nishida, E. 2002. JNK functions in the noncanonical Wnt pathway to regulate convergent extension movements in vertebrates. *EMBO Rep.* **3:** 69–75.
Yelon, D., Ticho, B., Halpern, M.E., Ruvinsky, I., Ho, R.K., Silver, L.M., and Stainier, D.Y. 2000. The bHLH transcription factor hand2 plays parallel roles in zebrafish heart and pectoral fin development. *Development* **127:** 2573–2582.